The effect of APOE ε4 allele on cholinesterase inhibitors in patients with Alzheimer's disease: Evaluation of the feasibility of resting state functional connectivity magnetic resonance imaging

Liang Wang MD, Jonathan Day, Catherine M. Roe PhD, Matthew R. Brier BS, Jewell B. Thomas BA, Tammie L. Benzinger MD, PhD, John C. Morris MD, and Beau M. Ances MD, PhD

Supplemental materials

Methods

Pre-processing of resting state fMRI data

The fMRI data were preprocessed as previously described [1]. Briefly, this included compensation for slice-dependent time shifts, elimination of systematic odd-even slice intensity differences due to interleaved acquisition and rigid body correction for head movement within and across runs. The data were intensity scaled (one multiplicative factor applied to all voxels of all frames within each run) to obtain a mode value of 1000 [2]. This procedure facilitated assessment of voxel-wise variance for purposes of quality assurance but did not affect computed correlations. Atlas transformation was achieved by composition of affine transforms connecting the fMRI volumes with the T2-weighted and MPRAGE structural images. Head movement correction was included in a single resampling that generated a volumetric time-series in $(3mm)^3$ atlas space.

Several additional preprocessing steps were carried out in preparation for correlation analysis. First, data were spatially smoothed with a 6-mm full width at half maximum Gaussian blur. Second, temporal low-pass filtering ($f < 0.1$ Hz) was applied to the time series of each voxel to remove high-frequency components. Third, head motion during resting state functional connectivity MRI acquisition impacts not only image position but also BOLD signal amplitude. Realignment corrects for image shift in space but does not affect the BOLD signal amplitude. Thus, head motion-related signal was removed by regression of six parameters generated from rigid body correction of head motion[3, 4]. Fourth, additional sources of spurious variance were removed from the data by linear regression: (1) the whole brain signal averaged from a mask region in atlas space; (2) signal from a ventricular ROI, and ROIs located in bilateral deep cerebral white matter. A salient characteristic of whole brain signal regression is that all subsequently computed correlations are effectively partial correlations of the first order controlling for widely shared variance [5].

Quality assurance (QA) of fMRI data

The QA procedures for fMRI data have been described in our previous work [6]. Briefly, for each individual, we assessed fMRI data quality by computing voxelwise root mean squared (rms) variance (s.d.) averaged over the whole brain. Individuals with a mean preprocessed fMRI signal s.d. > 2.5% (before nuisance regression) or rms displacement due to head motion exceeding 1.25 mm were excluded. In

addition, recent work[7, 8] has demonstrated that, even after regression of motion estimates, residual effect of head motion systematically impact functional correlation. To minimize the effect of head motion in the present study, we removed frames with high signal variance associated with head motion using a previously proposed method [7]. We originally applied these QA procedures to a larger sample of participants and excluded a total of 49 participants from that sample. A subset of that sample in which data regarding the nature history of AD medication were available is reported in the present work.

Results

Effects of APOE ε4 allele on RSN composite scores within untreated participants

APOE ε4 carriers had lower MMSE scores than non-carriers. Other demographic variables were not significantly different between the *APOE* ε4 carriers and non-carriers. *APOE* ε4 carriers had significantly lower composite scores in the DMN, DAN, CON and SMN compared to non-carriers (all $p < 0.05$). However, such effects were not significant after adjusting for the MMSE differences (all $p \geq 0.19$).

Effects of APOE ε4 allele on RSN composite scores within treated participants

APOE ε4 carriers were more likely to be female compared to non-carriers. Other demographic variables were not significantly different between the *APOE* ε4 carriers and non-carriers. A significant difference in composite scores was observed only in the SAL ($p < 0.05$) but not in other RSNs ($p \geq 0.27$) between *APOE* ε4 non-carriers and carriers. This effect was at a trend-level significance after adjusting for gender differences ($p = 0.08$).

Figure Legend

Figure S1. The distributions of pairwise correlations in the default mode network (DMN)

For each participant, pairwise correlations were computed using 9 *a priori*-defined DMN regions of interest. The frequency distributions of these correlation coefficients are displayed. See Supplemental Table S1 for abbreviations.

Supplemental Tables

Table S1 Peak locations of regions of interest

Regions of Interest	MNI Coordinates
Default mode network (DMN)	
Posterior Cingulate Cortex (PCC)	0,-51,29
Medial Prefrontal Cortex (mPFC)	0,61,22
Left Lateral Parietal (lLP)	-48,-66,34
Right Lateral Parietal (rLP)	53,-61,35
Left Inferior Temporal (liTmp)	-65,-22,-9
Right Inferior Temporal (riTmp)	61,-21,-12
Medial Thalamus (mdThal)	0,-9,7
Left Posterior Cerebellum (lpCBLM)	-28,-82,-32
Right Posteior Cerebellum (rpCBLM)	26,-89,-34
Dorsal Attention Network (DAN)	
Left front eye field (lFEF)	-29,-5,-55
Right Frontal Eye Field (rFEF)	31,-5,54
Left Posterior Intraparietal sulcus (lpIPS)	-26,-65,52
Right Posterior Intraparietal sulcus (rpIPS)	28,-65,51
Left Anterior Intraparietal sulcus (laIPS)	-45,-37,48
Right Anterior Intraparietal sulcus (raIPS)	43,-36,46
Left Middle Temporal (lMT)	-52,-66,-4
Right Middle Temporal (rMT)	55,-62,-7
Control Network (CON)	
Dorsal medial prefrontal cortex (dmPFC)	1,30,44
Left anterior (laPFC)	-45,50,-5
Right anterior PFC (raPFC)	46,51,-7
Left superior parietal (lSP)	-51,-50,49
Right superior Parietal (rSP)	53,-49,47
Salience Network (SAL)	
Dorsal anterior cingulate cortex (dACC)	1,26,34
Left anterior prefrontal cortex (laPFC)	35,51,27
Right anterior prefrontal cortex (raPFC)	-37,52,25
Left lateral parietal cortex (lLP)	-49,-51,45
Right lateral parietal cortex (rLP)	49,-51,45
Left Insula (lIns)	-42,6,4
Right Insula (rIns)	43,7,2
Sensory-Motor network (SMN)	
Left Motor Ctx (lMC)	-40,-23,53
Right Motor Ctx (rMC)	41,-22,48
Supplementary Motor Area (SMA)	1,-18,49
Left Primary Visual (lV1)	-8,-83,0
Right Primary Visual (rV1)	7,-83,0
Left Primary Audiotry (lA1)	-64,-28,13
Right Primary Auditory (rA1)	62,-24,13

Table S2 Demographics of the separate groups of APOE ε4 carriers (A) and non-carriers (B)

A.

Participants	Untreated	Treated	p value
	N = 11	N = 16	
Mean Age (SD), year	76.6 (6.7)	75.3 (4.2)	0.54
Age range, year	67-88	65-82	
Sex, %Male	36.4	31.3	1.00
Mean Education (SD), year	15.4 (3.0)	14.3 (2.8)	1.00
Mean MMSE (SD)	23.6 (3.8)	25.9 (2.8)	0.34
CDR (No. of 0.5/1)	8/3	13/3	0.66
Mean CDR sum box (SD)	2.6 (1.9)	3.1 (1.6)	0.43

B.

Participants	Untreated	Treated	p value
	N = 8	N = 9	
Mean Age (SD), year	74.8 (7.3)	78.0 (6.3)	0.34
Age range, year	64-82	65-84	
Sex, %Male	50.0	77.8	0.34
Mean Education (SD), year	13.8 (2.5)	15.4 (2.7)	0.20
Mean MMSE (SD)	28.0 (1.3)	27.4 (3.4)	0.67
CDR (No. of 0.5/1)	8/0	8/1	1.00
Mean CDR sum box (SD)	1.9 (0.9)	2.4 (1.5)	0.46

SD: standard deviation, MMSE: mini-mental state examination, for which the range of scores is from 30 (“best”) to 0 (“worst”), CDR: Clinical Dementia Rating, for which CDR 0.5 CDR 1 indicate very mild and mild AD respectively, CDR sum of boxes (the sum of individual CDR domain scores) range from 0 to 18, with lower scores indicating better performance. APOE: Apolipoprotein E

REFERENCES

1. Shulman GL, Pope DL, Astafiev SV, McAvoy MP, Snyder AZ, Corbetta M. Right hemisphere dominance during spatial selective attention and target detection occurs outside the dorsal frontoparietal network. *The Journal of neuroscience : the official journal of the Society for Neuroscience.* 2010;30(10):3640-3651.

2. Ojemann JG, Buckner RL, Corbetta M, Raichle ME. Imaging studies of memory and attention. *Neurosurgery clinics of North America.* 1997;8(3):307-319.

3. Vincent JL, Snyder AZ, Fox MD, Shannon BJ, Andrews JR, Raichle ME, Buckner RL. Coherent spontaneous activity identifies a hippocampal-parietal memory network. *J Neurophysiol.* 2006;96(6):3517-3531.

4. Van Dijk KR, Hedden T, Venkataraman A, Evans KC, Lazar SW, Buckner RL. Intrinsic functional connectivity as a tool for human connectomics: theory, properties, and optimization. *J Neurophysiol.* 2010;103(1):297-321.

5. Fox MD, Zhang D, Snyder AZ, Raichle ME. The global signal and observed anticorrelated resting state brain networks. *J Neurophysiol.* 2009;101(6):3270-3283.

6. Wang L, Roe CM, Snyder AZ, Brier MR, Thomas JB, Xiong C, Benzinger TL, Morris JC, Ances BM. Alzheimer's disease family history impacts resting state functional connectivity. *Annals of neurology.* 2012;In press.

7. Power JD, Barnes KA, Snyder AZ, Schlaggar BL, Petersen SE. Spurious but systematic correlations in functional connectivity MRI networks arise from subject motion. *Neuroimage.* 2012;59(3):2142-2154.

8. Van Dijk KR, Sabuncu MR, Buckner RL. The influence of head motion on intrinsic functional connectivity MRI. *Neuroimage.* 2012;59(1):431-438.

The effect of APOE ε4 allele on cholinesterase inhibitors in patients with Alzheimer's disease: Evaluation of the feasibility of resting state functional connectivity magnetic resonance imaging

Liang Wang MD, Jonathan Day, Catherine M. Roe PhD, Matthew R. Brier BS, Jewell B. Thomas BA, Tammie L. Benzinger MD, PhD, John C. Morris MD, and Beau M. Ances MD, PhD

Supplemental materials

Methods

Pre-processing of resting state fMRI data

The fMRI data were preprocessed as previously described [1]. Briefly, this included compensation for slice-dependent time shifts, elimination of systematic odd-even slice intensity differences due to interleaved acquisition and rigid body correction for head movement within and across runs. The data were intensity scaled (one multiplicative factor applied to all voxels of all frames within each run) to obtain a mode value of 1000 [2]. This procedure facilitated assessment of voxel-wise variance for purposes of quality assurance but did not affect computed correlations. Atlas transformation was achieved by composition of affine transforms connecting the fMRI volumes with the T2-weighted and MPRAGE structural images. Head movement correction was included in a single resampling that generated a volumetric time-series in $(3mm)^3$ atlas space.

Several additional preprocessing steps were carried out in preparation for correlation analysis. First, data were spatially smoothed with a 6-mm full width at half maximum Gaussian blur. Second, temporal low-pass filtering ($f < 0.1$ Hz) was applied to the time series of each voxel to remove high-frequency components. Third, head motion during resting state functional connectivity MRI acquisition impacts not only image position but also BOLD signal amplitude. Realignment corrects for image shift in space but does not affect the BOLD signal amplitude. Thus, head motion-related signal was removed by regression of six parameters generated from rigid body correction of head motion[3, 4]. Fourth, additional sources of spurious variance were removed from the data by linear regression: (1) the whole brain signal averaged from a mask region in atlas space; (2) signal from a ventricular ROI, and ROIs located in bilateral deep cerebral white matter. A salient characteristic of whole brain signal regression is that all subsequently computed correlations are effectively partial correlations of the first order controlling for widely shared variance [5].

Quality assurance (QA) of fMRI data

The QA procedures for fMRI data have been described in our previous work [6]. Briefly, for each individual, we assessed fMRI data quality by computing voxelwise root mean squared (rms) variance (s.d.) averaged over the whole brain. Individuals with a mean preprocessed fMRI signal s.d. > 2.5% (before nuisance regression) or rms displacement due to head motion exceeding 1.25 mm were excluded. In

addition, recent work[7, 8] has demonstrated that, even after regression of motion estimates, residual effect of head motion systematically impact functional correlation. To minimize the effect of head motion in the present study, we removed frames with high signal variance associated with head motion using a previously proposed method [7]. We originally applied these QA procedures to a larger sample of participants and excluded a total of 49 participants from that sample. A subset of that sample in which data regarding the nature history of AD medication were available is reported in the present work.

Results

Effects of APOE ε4 allele on RSN composite scores within untreated participants

APOE ε4 carriers had lower MMSE scores than non-carriers. Other demographic variables were not significantly different between the *APOE* ε4 carriers and non-carriers. *APOE* ε4 carriers had significantly lower composite scores in the DMN, DAN, CON and SMN compared to non-carriers (all $p < 0.05$). However, such effects were not significant after adjusting for the MMSE differences (all $p \geq 0.19$).

Effects of APOE ε4 allele on RSN composite scores within treated participants

APOE ε4 carriers were more likely to be female compared to non-carriers. Other demographic variables were not significantly different between the *APOE* ε4 carriers and non-carriers. A significant difference in composite scores was observed only in the SAL ($p < 0.05$) but not in other RSNs ($p \geq 0.27$) between *APOE* ε4 non-carriers and carriers. This effect was at a trend-level significance after adjusting for gender differences ($p = 0.08$).

Figure Legend

Figure S1. The distributions of pairwise correlations in the default mode network (DMN)

For each participant, pairwise correlations were computed using 9 *a priori*-defined DMN regions of interest. The frequency distributions of these correlation coefficients are displayed. See Supplemental Table S1 for abbreviations.

Supplemental Tables

Table S1 Peak locations of regions of interest

Regions of Interest	MNI Coordinates
Default mode network (DMN)	
Posterior Cingulate Cortex (PCC)	0,-51,29
Medial Prefrontal Cortex (mPFC)	0,61,22
Left Lateral Parietal (lLP)	-48,-66,34
Right Lateral Parietal (rLP)	53,-61,35
Left Inferior Temporal (liTmp)	-65,-22,-9
Right Inferior Temporal (riTmp)	61,-21,-12
Medial Thalamus (mdThal)	0,-9,7
Left Posterior Cerebellum (lpCBLM)	-28,-82,-32
Right Posteior Cerebellum (rpCBLM)	26,-89,-34
Dorsal Attention Network (DAN)	
Left front eye field (lFEF)	-29,-5,-55
Right Frontal Eye Field (rFEF)	31,-5,54
Left Posterior Intraparietal sulcus (lpIPS)	-26,-65,52
Right Posterior Intraparietal sulcus (rpIPS)	28,-65,51
Left Anterior Intraparietal sulcus (laIPS)	-45,-37,48
Right Anterior Intraparietal sulcus (raIPS)	43,-36,46
Left Middle Temporal (lMT)	-52,-66,-4
Right Middle Temporal (rMT)	55,-62,-7
Control Network (CON)	
Dorsal medial prefrontal cortex (dmPFC)	1,30,44
Left anterior (laPFC)	-45,50,-5
Right anterior PFC (raPFC)	46,51,-7
Left superior parietal (lSP)	-51,-50,49
Right superior Parietal (rSP)	53,-49,47
Salience Network (SAL)	
Dorsal anterior cingulate cortex (dACC)	1,26,34
Left anterior prefrontal cortex (laPFC)	35,51,27
Right anterior prefrontal cortex (raPFC)	-37,52,25
Left lateral parietal cortex (lLP)	-49,-51,45
Right lateral parietal cortex (rLP)	49,-51,45
Left Insula (lIns)	-42,6,4
Right Insula (rIns)	43,7,2
Sensory-Motor network (SMN)	
Left Motor Ctx (lMC)	-40,-23,53
Right Motor Ctx (rMC)	41,-22,48
Supplementary Motor Area (SMA)	1,-18,49
Left Primary Visual (lV1)	-8,-83,0
Right Primary Visual (rV1)	7,-83,0
Left Primary Audiotry (lA1)	-64,-28,13
Right Primary Auditory (rA1)	62,-24,13

Table S2 Demographics of the separate groups of APOE ε4 carriers (A) and non-carriers (B)

A.

Participants	Untreated	Treated	p value
	N = 11	N = 16	
Mean Age (SD), year	76.6 (6.7)	75.3 (4.2)	0.54
Age range, year	67-88	65-82	
Sex, %Male	36.4	31.3	1.00
Mean Education (SD), year	15.4 (3.0)	14.3 (2.8)	1.00
Mean MMSE (SD)	23.6 (3.8)	25.9 (2.8)	0.34
CDR (No. of 0.5/1)	8/3	13/3	0.66
Mean CDR sum box (SD)	2.6 (1.9)	3.1 (1.6)	0.43

B.

Participants	Untreated	Treated	p value
	N = 8	N = 9	
Mean Age (SD), year	74.8 (7.3)	78.0 (6.3)	0.34
Age range, year	64-82	65-84	
Sex, %Male	50.0	77.8	0.34
Mean Education (SD), year	13.8 (2.5)	15.4 (2.7)	0.20
Mean MMSE (SD)	28.0 (1.3)	27.4 (3.4)	0.67
CDR (No. of 0.5/1)	8/0	8/1	1.00
Mean CDR sum box (SD)	1.9 (0.9)	2.4 (1.5)	0.46

SD: standard deviation, MMSE: mini-mental state examination, for which the range of scores is from 30 (“best”) to 0 (“worst”), CDR: Clinical Dementia Rating, for which CDR 0.5 CDR 1 indicate very mild and mild AD respectively, CDR sum of boxes (the sum of individual CDR domain scores) range from 0 to 18, with lower scores indicating better performance. APOE: Apolipoprotein E

REFERENCES

1. Shulman GL, Pope DL, Astafiev SV, McAvoy MP, Snyder AZ, Corbetta M. Right hemisphere dominance during spatial selective attention and target detection occurs outside the dorsal frontoparietal network. *The Journal of neuroscience : the official journal of the Society for Neuroscience.* 2010;30(10):3640-3651.

2. Ojemann JG, Buckner RL, Corbetta M, Raichle ME. Imaging studies of memory and attention. *Neurosurgery clinics of North America.* 1997;8(3):307-319.

3. Vincent JL, Snyder AZ, Fox MD, Shannon BJ, Andrews JR, Raichle ME, Buckner RL. Coherent spontaneous activity identifies a hippocampal-parietal memory network. *J Neurophysiol.* 2006;96(6):3517-3531.

4. Van Dijk KR, Hedden T, Venkataraman A, Evans KC, Lazar SW, Buckner RL. Intrinsic functional connectivity as a tool for human connectomics: theory, properties, and optimization. *J Neurophysiol.* 2010;103(1):297-321.

5. Fox MD, Zhang D, Snyder AZ, Raichle ME. The global signal and observed anticorrelated resting state brain networks. *J Neurophysiol.* 2009;101(6):3270-3283.

6. Wang L, Roe CM, Snyder AZ, Brier MR, Thomas JB, Xiong C, Benzinger TL, Morris JC, Ances BM. Alzheimer's disease family history impacts resting state functional connectivity. *Annals of neurology.* 2012;In press.

7. Power JD, Barnes KA, Snyder AZ, Schlaggar BL, Petersen SE. Spurious but systematic correlations in functional connectivity MRI networks arise from subject motion. *Neuroimage.* 2012;59(3):2142-2154.

8. Van Dijk KR, Sabuncu MR, Buckner RL. The influence of head motion on intrinsic functional connectivity MRI. *Neuroimage.* 2012;59(1):431-438.

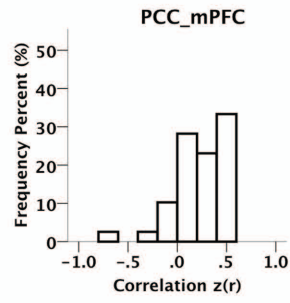
PCC_mPFC
Frequency Percent (%)
Correlation z(r)

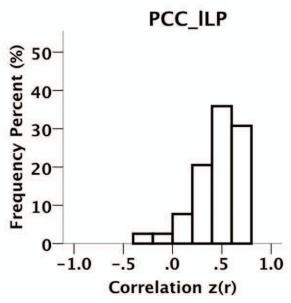
PCC_lLP
Frequency Percent (%)
Correlation z(r)

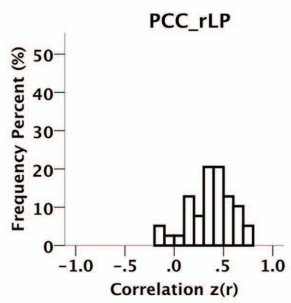
PCC_rLP
Frequency Percent (%)
Correlation z(r)

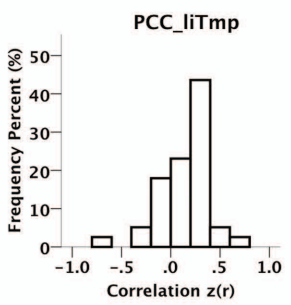
PCC_liTmp
Frequency Percent (%)
Correlation z(r)

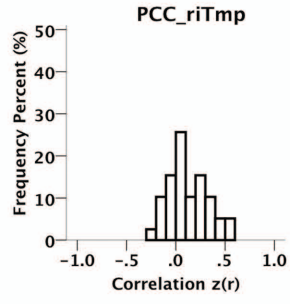
PCC_riTmp
Frequency Percent (%)
Correlation z(r)

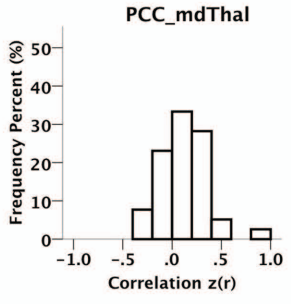
PCC_mdThal
Frequency Percent (%)
Correlation z(r)

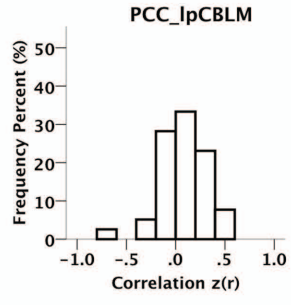
PCC_lpCBLM
Frequency Percent (%)
Correlation z(r)

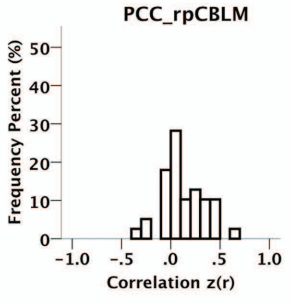
PCC_rpCBLM
Frequency Percent (%)
Correlation z(r)

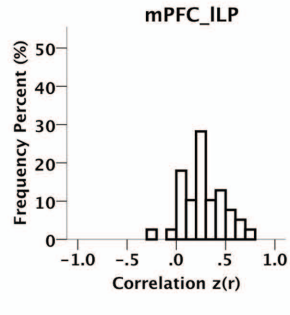
mPFC_lLP
Frequency Percent (%)
Correlation z(r)

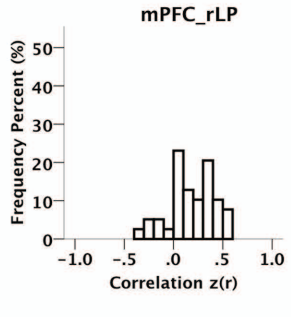
mPFC_rLP
Frequency Percent (%)
Correlation z(r)

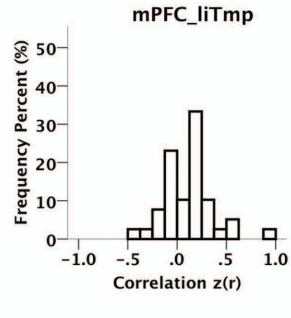
mPFC_liTmp
Frequency Percent (%)
Correlation z(r)

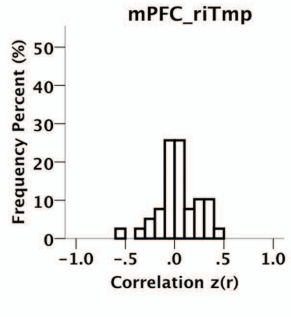
mPFC_riTmp
Frequency Percent (%)
Correlation z(r)

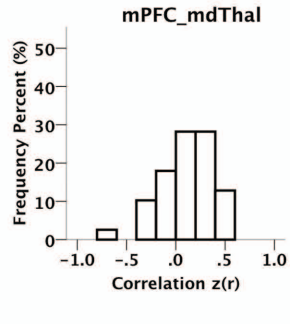
mPFC_mdThal
Frequency Percent (%)
Correlation z(r)

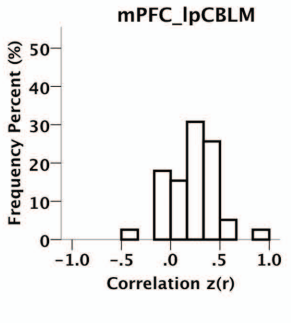
mPFC_lpCBLM
Frequency Percent (%)
Correlation z(r)

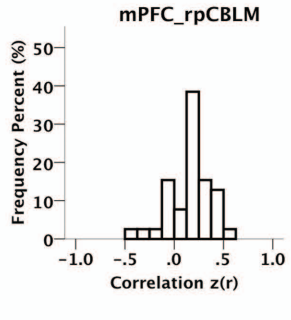
mPFC_rpCBLM
Frequency Percent (%)
Correlation z(r)

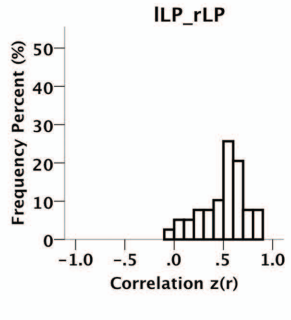
lLP_rLP
Frequency Percent (%)
Correlation z(r)

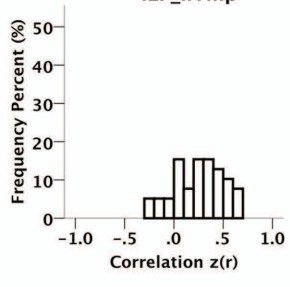
lLP_liTmp
Frequency Percent (%)
Correlation z(r)

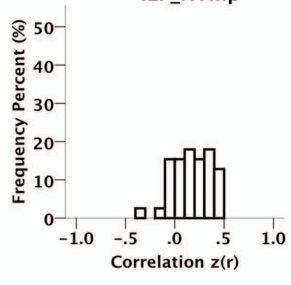
lLP_riTmp
Frequency Percent (%)
Correlation z(r)

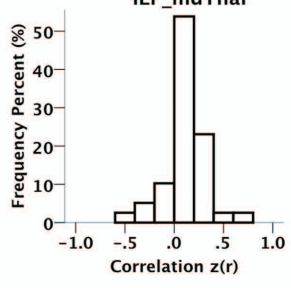
lLP_mdThal
Frequency Percent (%)
Correlation z(r)

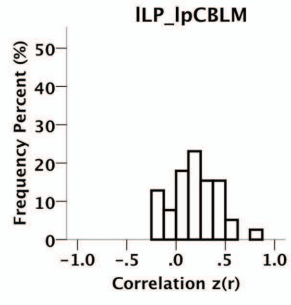
lLP_lpCBLM
Frequency Percent (%)
Correlation z(r)

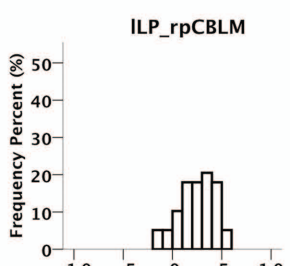
lLP_rpCBLM
Frequency Percent (%)
Correlation z(r)

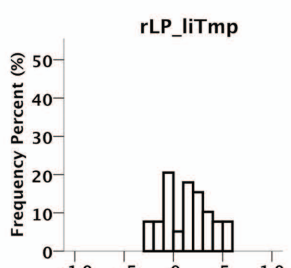
rLP_liTmp
Frequency Percent (%)
Correlation z(r)

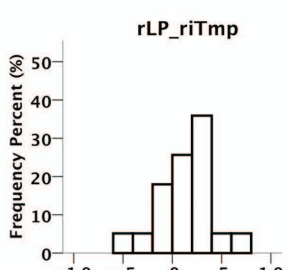
rLP_riTmp
Frequency Percent (%)
Correlation z(r)

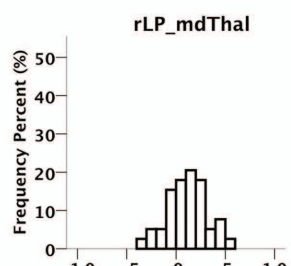
rLP_mdThal
Frequency Percent (%)
Correlation z(r)

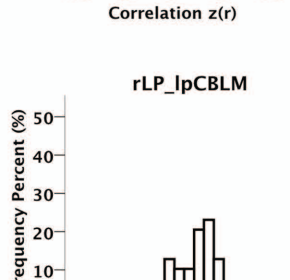
rLP_lpCBLM
Frequency Percent (%)
Correlation z(r)

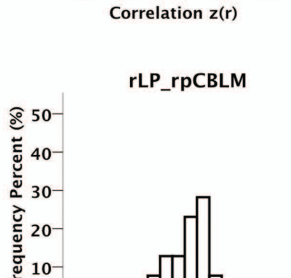
rLP_rpCBLM
Frequency Percent (%)
Correlation z(r)

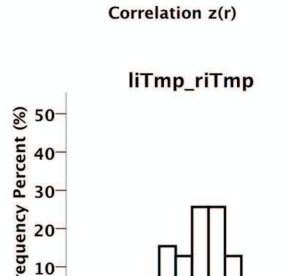
liTmp_riTmp
Frequency Percent (%)
Correlation z(r)

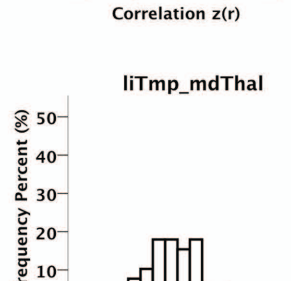
liTmp_mdThal
Frequency Percent (%)
Correlation z(r)

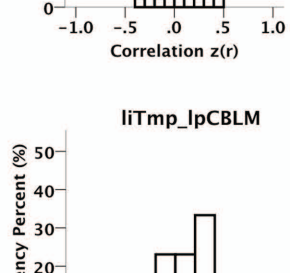
liTmp_lpCBLM
Frequency Percent (%)
Correlation z(r)

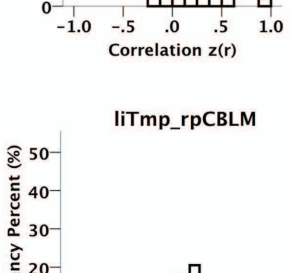
liTmp_rpCBLM
Frequency Percent (%)
Correlation z(r)

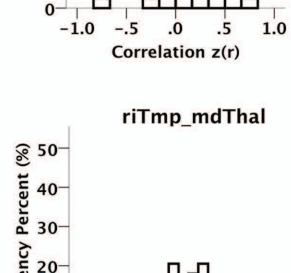
riTmp_mdThal
Frequency Percent (%)
Correlation z(r)

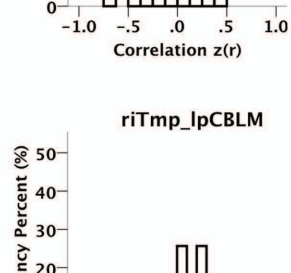
riTmp_lpCBLM
Frequency Percent (%)
Correlation z(r)

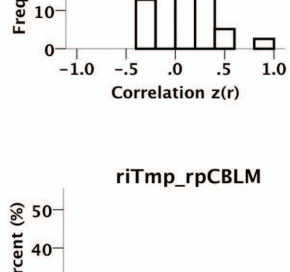
riTmp_rpCBLM
Frequency Percent (%)
Correlation z(r)

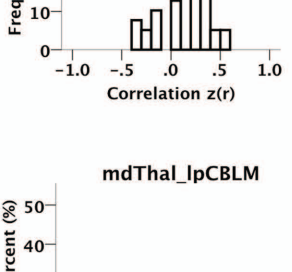
mdThal_lpCBLM
Frequency Percent (%)
Correlation z(r)

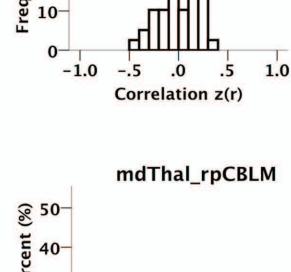
mdThal_rpCBLM
Frequency Percent (%)
Correlation z(r)

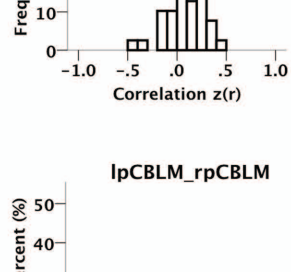
lpCBLM_rpCBLM
Frequency Percent (%)
Correlation z(r)

PCC_mPFC

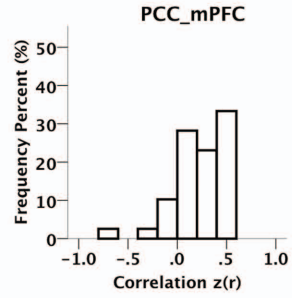

PCC_lLP

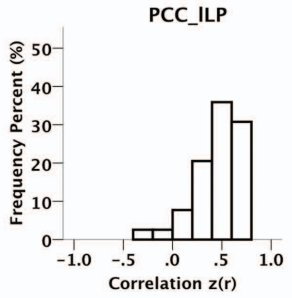

PCC_rLP

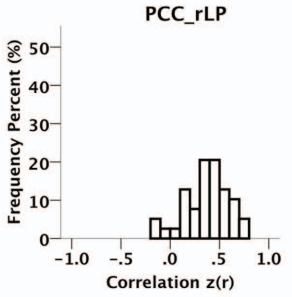

PCC_liTmp

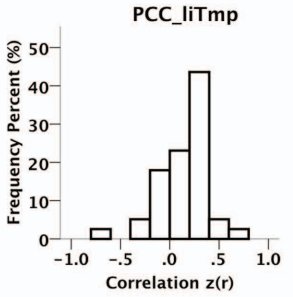

PCC_riTmp

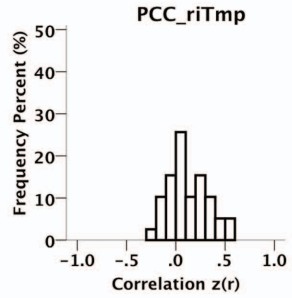

PCC_mdThal

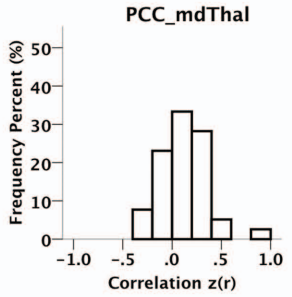

PCC_lpCBLM

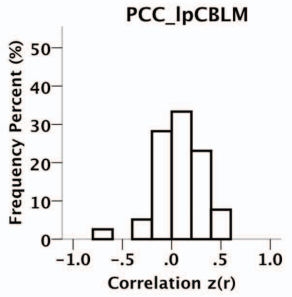

PCC_rpCBLM

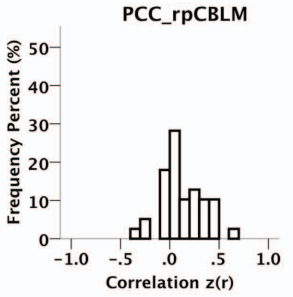

mPFC_lLP

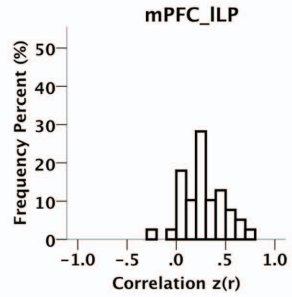

mPFC_rLP

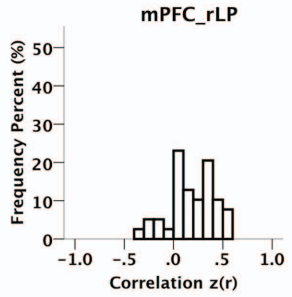

mPFC_liTmp

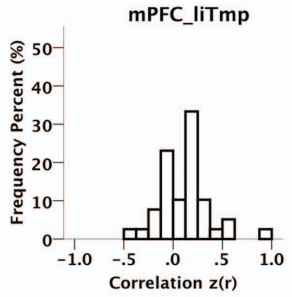

mPFC_riTmp

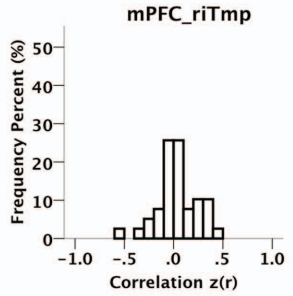

mPFC_mdThal

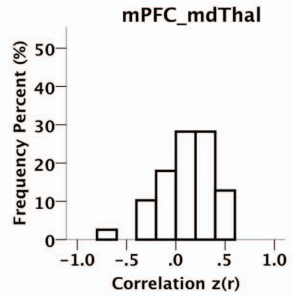

mPFC_lpCBLM

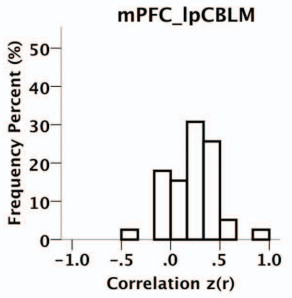

mPFC_rpCBLM

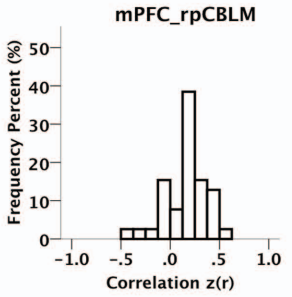

lLP_rLP

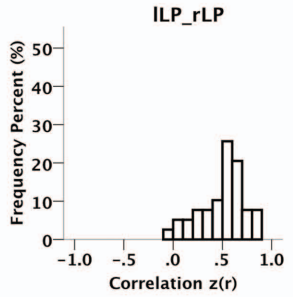

lLP_liTmp

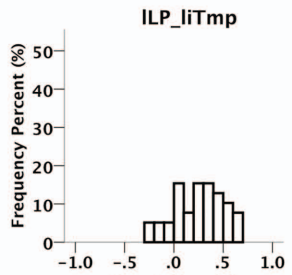

lLP_riTmp

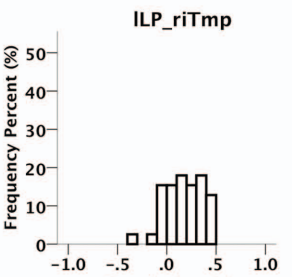

lLP_mdThal

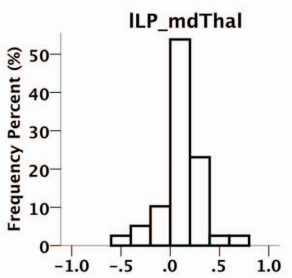

lLP_lpCBLM

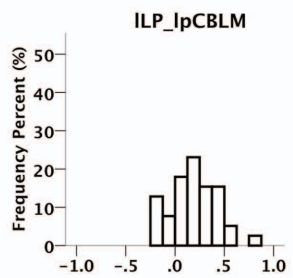

lLP_rpCBLM

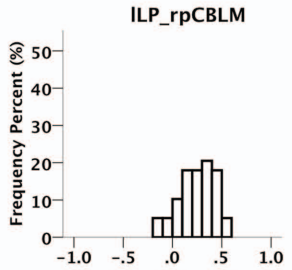

rLP_liTmp

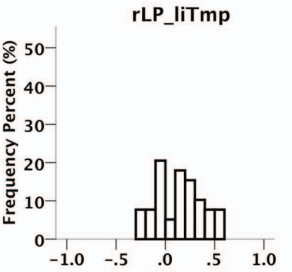

rLP_riTmp

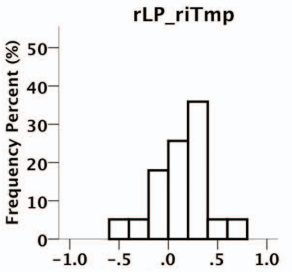

rLP_mdThal

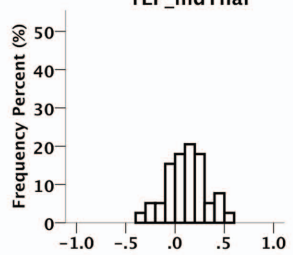

rLP_lpCBLM

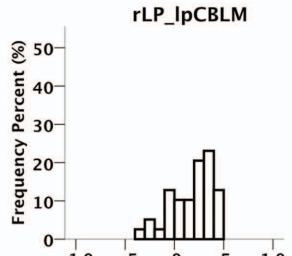

rLP_rpCBLM

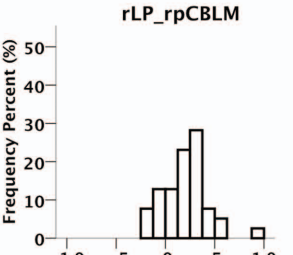

liTmp_riTmp

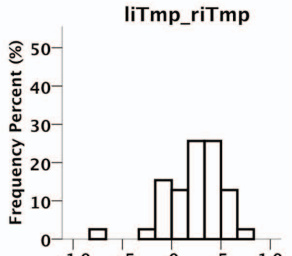

liTmp_mdThal

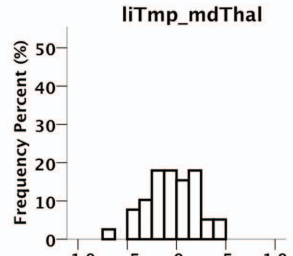

liTmp_lpCBLM

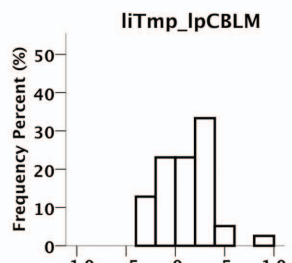

liTmp_rpCBLM

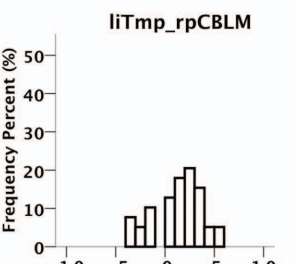

riTmp_mdThal

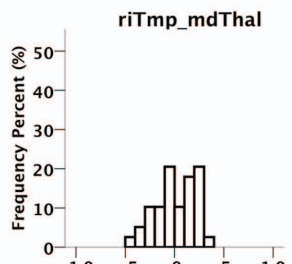

riTmp_lpCBLM

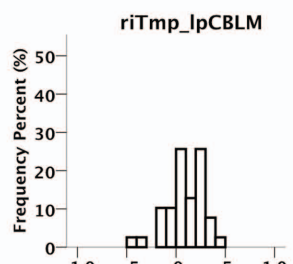

riTmp_rpCBLM

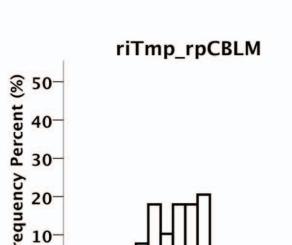

mdThal_lpCBLM

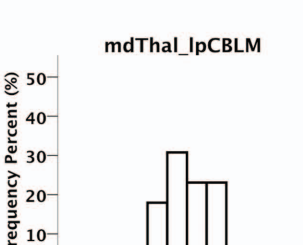

mdThal_rpCBLM

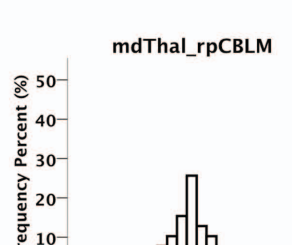

lpCBLM_rpCBLM